Research Paper

# MgSO₄ as a novel hypothermia infusion solution promotes ischemic stroke recovery through Ca²⁺ regulation of neurovascular units

Yang Zhang[1,2,#], Miaowen Jiang[3,#], Ming Wei[4,#], Chuanjie Wu[1,2,#], Yiming Huang[1,2], Baoying Song[1,2], Yi Xu[1,2], Hongkang Zhang[5], Yunong Shen[5], Di Wu[2,✉], Yufeng Zheng[5,✉], Ming Li[2,✉], Xunming Ji[2,3,6,✉]

1. Department of Neurology, Xuanwu Hospital, Capital Medical University, Beijing, China.
2. China-America Institute of Neurology, Xuanwu Hospital, Capital Medical University, Beijing, China.
3. Beijing Institute of Brain Disorders, Capital Medical University, Beijing, China.
4. Department of Neurosurgery, Tianjin Huanhu Hospital, Tianjin, China.
5. School of Materials Science and Engineering, Peking University; Beijing, China.
6. Department of Neurosurgery, Xuanwu Hospital, Capital Medical University, Beijing, China.

\# These authors contributed equally to this work.

✉ Corresponding authors: Prof. Xunming Ji, Department of Neurosurgery, Xuanwu Hospital, Capital Medical University, No. 45, Changchun Street, Xicheng District, Beijing, China. Email: jixm@ccmu.edu.cn. Prof. Ming Li, China-America Institute of Neurology, Xuanwu Hospital, Capital Medical University, No. 45, Changchun Street, Xicheng District, Beijing, China. Email: liming@xwhosp.org. Prof. Yufeng Zheng, School of Materials Science and Engineering, Peking University; No. 5 Yiheyuan Road, Haidian District, Beijing, China. Email: yfzheng@pku.edu.cn. Prof. Di Wu, China-America Institute of Neurology, Xuanwu Hospital, Capital Medical University, No. 45, Changchun Street, Xicheng District, Beijing, China. Email: seadi_wu@163.com.

## Abstract

The neuroprotection of acute ischemic stroke (AIS) patients to alleviate the reperfusion injury is a long-standing problem. Although the intra-arterial selective cooling saline infusion (IA-SCSI) is a promising technique to improve the outcome of AIS, the clinical results are not sufficiently satisfactory. Magnesium-containing solutions such as magnesium sulfate (MgSO₄) can protect cells by modulating the intracellular Ca²⁺ content in damaged cells, suggesting that they could be hypothermia infusion solution. In this study, we hypothesized that MgSO₄, as a novel hypothermia infusion solution (IA-SCMI), can promote AIS recovery.

**Methods:** First, IA-SCMI was performed in rats subjected to the middle cerebral artery occlusion. The effect of combined hypothermia and MgSO₄ treatment on different neurovascular (NVU) cells after oxygen-glucose deprivation/reoxygenation (OGD/R) injury was examined.

**Results:** Compared with the IA-SCSI or IA-MgSO₄ infusion alone, IA-SCMI offered the best protective effect by improving neurological defects, and alleviating brain integrity damage and CBF reduction. Meanwhile, *in vitro* results revealed that the combination of hypothermia and MgSO₄ provided maximum protection to the NVU cells, and this protective effect was mainly achieved through the regulation of Ca²⁺ homeostasis in different cells.

**Conclusion:** MgSO₄ may be a promising hypothermia infusion solution to facilitate the recovery of neurological function in AIS patients.

Keywords: magnesium sulfate, hypothermia, ischemic stroke, neurovascular units, calcium

## Introduction

Acute ischemic stroke (AIS) is the leading cause of morbidity and mortality worldwide [1, 2]. The validation and widespread adoption of thrombectomy and thrombolysis have ushered in the era of reperfusion therapy for AIS [3]. However, nearly half of patients with complete proximal large artery recanalization do not achieve functional independence, due to potential ischemia/reperfusion

(I/R) injury [4]. Therefore, it is essential to develop alternative strategies in combination with successful recanalization to enhance patient outcomes.

Hypothermia therapy is a long-standing method for treating brain injury including ischemic stroke. It confers neuroprotective effects by modulating diverse neurovascular units (NVUs) [5, 6] such as neural protection and blood-brain barrier (BBB) restoration. Owing to its serious systemic side effects [7], whole body hypothermia is increasingly being replaced by selective brain cooling like ice cap cooling [8] and transnasal cooling [9]. Furthermore, advances in endovascular treatment have led to the development of a more precise technique, intra-arterial selective cooling saline infusion (IA-SCSI) [10, 11]. This method has been validated in AIS model of various animals, such as rats [12] and rhesus monkeys [13]. However, the clinical outcomes are not sufficiently satisfactory [14]. Besides, hypothermia has been indicated to reduces cerebral capillary blood flow, thus maybe hinder microcirculation reperfusion after recanalization [15]. Therefore, it is imperative to formulate new perfusion solutions that can replace saline to facilitate neuroprotection and prevent the microcirculation damage induced by hypothermia. Magnesium-containing solutions seem to be a good candidate, with previous studies showing that surface hypothermia combined with intravenous infusion of $Mg^{2+}$ promotes AIS recovery [16, 17].

Magnesium-containing solutions like magnesium sulfate ($MgSO_4$) and magnesium chloride ($MgCl_2$) exert multiple neuroprotective effects [18]. Briefly, $Mg^{2+}$ as an endogenous antagonist of the calcium channel might decrease brain excitotoxicity and cell death induced by calcium overload following nervous system injury [19]. Studies have demonstrated that $Mg^{2+}$ affects the permeability of the BBB and inhibits inflammatory response [20, 21]. Moreover, $Mg^{2+}$ could block calcium channels to prevent the synthesis of endothelin-1, inhibit myosin light chain kinase activation in vascular diameter regulating cells and attenuate vasospasm and contraction, leading to increased cerebral blood flow [22]. Therefore, $Mg^{2+}$-containing solutions, with multiple NVU regulatory effects on calcium, seems to be a good choice for intra-arterial selective cooling infusion. Furthermore, considering that hypothermia therapy can regulate calcium channels [23, 24], the respective co-regulatory effect of the combination of hypothermia and $Mg^{2+}$ therapy on the calcium ion of different NVU cells should be focused on, which has never been investigated before because most predecessors only observed the impact of hypothermia or $Mg^{2+}$ on a single type of cell.

In this study, we used $MgSO_4$ as novel intra-arterial selective cooling infusion solution (IA-SCMI) to determine whether this therapeutic strategy could provide additional neuroprotection. To test this hypothesis, IA-SCMI was performed in rats subjected to transient middle cerebral artery occlusion (MCAO) and the behaviors of rats were tested. In addition, the degree of neuron damage, BBB breakdown and cerebral blood reflow (CBF) was evaluated. Finally, oxygen-glucose deprivation/reoxygenation (OGD/R) models were established *in vitro* for different NVU member cells (neurons, microvessel endothelial cells (ECs) and pericytes) which were then treated with hypothermia and $Mg^{2+}$ to investigate the multiple cerebral protective mechanisms of the combination therapy, especially from the perspective of calcium ion regulation.

## Methods

### Animal and live experimental process

Male mature Sprague-Dawley (SD) rats weighing between 280 and 320 g were used in all experiments. All experimental procedures were approved by Institutional Animal Investigation Committee of Capital Medical University. The animal treatments were conducted following the National Institutes of Health's guidelines for the Care and Use of Laboratory Animals.

Procedurally, the cooling effect of IA-SCMI was explored *in vivo*, and the live experiments were divided into two parts: behavioral testing and histological evaluation. Behavioral tests included the modified neuropathy symptom score (mNSS), rotarod test, and adhesive removal test. The rats were trained one day before surgery to obtain baseline scores, and then tested on day 1, 3, 5, 7, 10, and 14 after operation. All tests were supervised by the same person, who was blinded to the treatment groups. Histological evaluation was conducted to assess neural integrity, BBB damage, and CBF. Neural cell damage was evaluated through short-term (one day post-surgery) assessment of cerebral infarction volume using triphenyltetrazolium chloride (TTC) staining and long-term evaluation of neural damage using Nissl staining seven days post-surgery. BBB damage was assessed on the third day post-surgery using Evans blue (EB) staining and brain water content measurement. CBF was continuously monitored before and during the MCAO, and within one day after reperfusion. The procedure of live experiments is shown in Figure 1A.
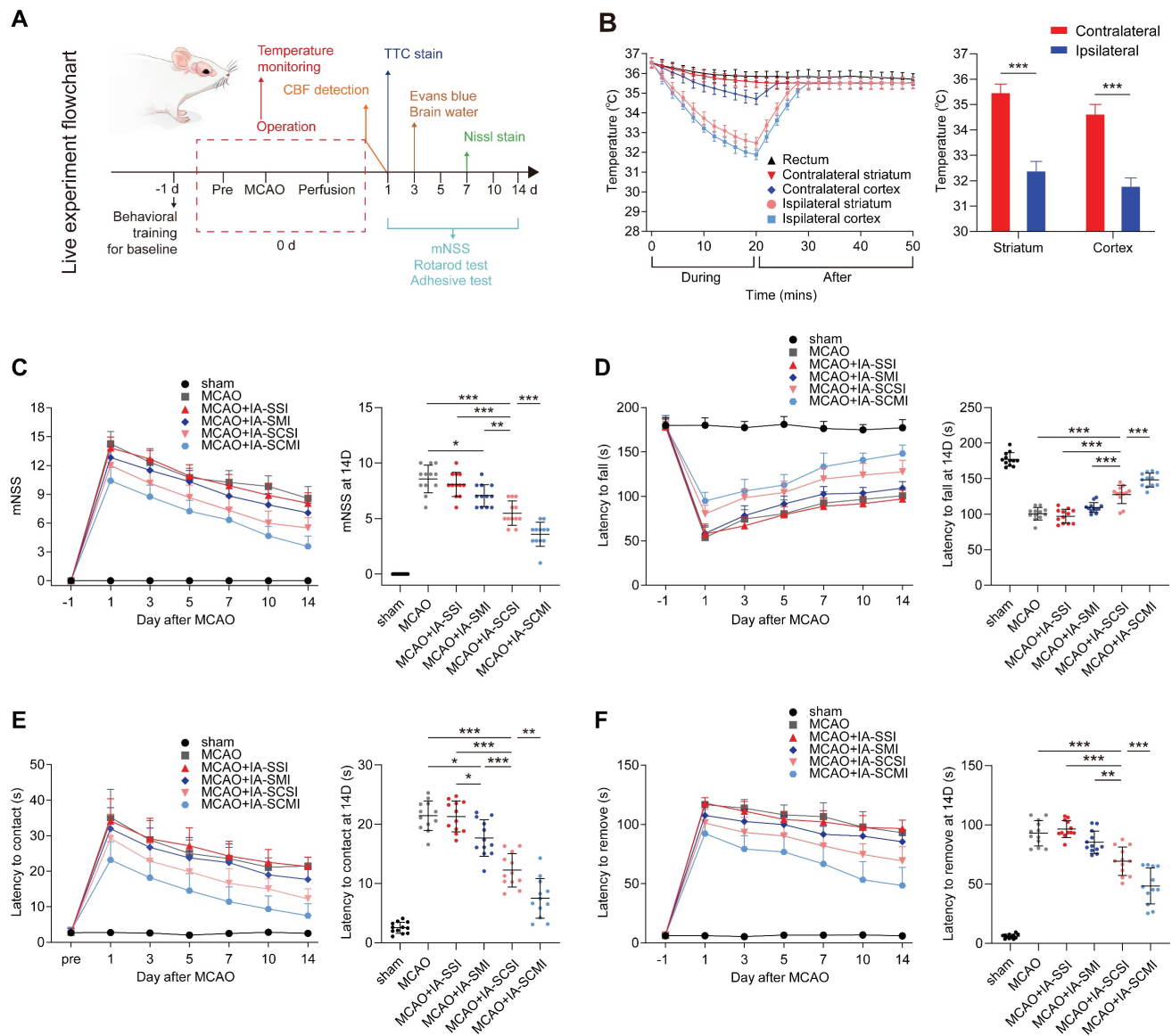
**Figure 1.** The *in vivo* cooling and neurological protection effect of IA-SCMI. (A) The flow chart of the live experiment. (B) The cooling effect of IA on the ipsilateral and contralateral cortex and striatum (n=5). (C) mNSS score (n=12). (D) Rotarod test (n=12). (E-F) Adhesive removal test (n=12). * $p < 0.05$, ** $p < 0.01$, *** $p < 0.001$.

## MCAO model

To mimic AIS I/R injury, we employed a transient MCAO procedure, as commonly described in the literature [25]. Five percent enflurane (RWD Life Science Co., LTD, China) was used for anesthesia, followed by maintenance with 1% to 3% enflurane. The skin of the rat's neck was shaved and disinfected, followed by creation of a longitudinal skin incision to expose the right common carotid artery (CCA), external carotid artery (ECA), and internal carotid artery (ICA). A tiny cut was made in the ECA, and a thread (RWD Life Science Co., LTD, China) was put through ECA and ICA to the right MCA's beginning (Figure S1A). After occlusion for 2 h, the thread was removed to achieve reperfusion of MCA.

## Intra-arterial selective infusion

Intra-arterial selective infusion (IA-SI) involved the infusion of 10 mL of different solutions, administered at the onset of reperfusion following a previously published method [26]. Rats in the four groups were subjected to IA-SI as follows: normothermic saline group (IA-SSI), normothermic $MgSO_4$ (3.6 mg/ml, Aladdin Biochemical Technology Co., Ltd, China) group (IA-SMI) [27], hypothermic (4°C) saline group (IA-SCSI), hypothermic $MgSO_4$ group (IA-SCMI). A small incision was created in the right ECA of each rat. This incision was used to advance a modified PE-10 catheter to reach the ICA. Subsequently, the solution was infused at a constant speed for 20 min using an injection pump (Figure S1B-C). Evaluating rats' tolerance to IA-SI was based

on measurements of some physiological parameters including the mean arterial blood pressure (MABP), heart rate and arterial oxygen partial pressure ($pO_2$) and arterial carbon dioxide partial pressure ($pCO_2$) before, during and after the IA-SI. The MABP and heart rate were recorded using an Automated Non-Invasive Blood Pressure Recording Tail-Cuff system (Softron, Japan). $pO_2$ and $pCO_2$ were determined using arterial blood collecting from the femoral artery of rats with a blood gas analyzer (Cornley, China).

## Brain and core temperature monitoring

Brain and rectal temperatures were continuously monitored before reperfusion, during and after IA-SI treatment using superfine temperature-sensor wires connected to a thermometer (Aidiwen Co., Ltd, China) as described previously (Figure S1C-D) [28, 29]. For brain temperature, wires were placed 3 mm lateral to the bregma, 4 mm in depth (striatum temperature), and 3 mm lateral and 3 mm posterior to the bregma, 2 mm in depth (cortical temperature), respectively. The core temperature was monitored by inserting wires into the rectum. To maintain core temperature, rats were placed on a feedback-regulated heating pad (RWD Life Science Co., LTD, China) during operation.

## Neurological behavioral tests

Neurological behavioral tests, including mNSS score, rotarod test, and adhesive removal test, were performed at the same time of day to control for circadian rhythm effects on behavior. The mNSS comprised assessments of motor function, sensory function, reflexes, balance, and abnormal movements [30], with scores ranging from 0 to 18 (normal score: 0; maximal deficiency score: 18). The details of the mNSS scoring procedure are presented in Table S1. In the rotarod test [30, 31], rats were placed on an accelerating rotating rod (RWD Life Science Co., LTD, China) and their latency to fall was measured. The rod speed was gradually increased from 4 to 40 rpm over 5 minutes. For the adhesive removal test [32], a piece of sticky tape was applied to the rat's left paw, and the time taken to remove the tape was recorded. If rats were unable to remove the tape within the allotted time limit of 2 min, the removal time was recorded as 2 min.

## Infarct volume

The rats were transcardially perfused with phosphate-buffered saline (PBS) and brains were collected. Brains were cut into five 2-mm sections and stained with 2% TTC (wt/vol in PBS, Solarbio Bioscience & Technology Co., LTD, China) for 20 min at 37°C to measure the infarct volume. After capturing images of the brain slices, the infarct volume ratio was calculated using ImageJ software (National Institutes of Health, USA) using the following formula: infarct volume ratio = (contralateral hemisphere area - noninfarcted area of the ipsilateral hemisphere) / contralateral hemisphere area.

## Neuron damage

The neuron damage was evaluated by performing Nissl staining on brain slices according to previous descriptions [33, 34]. The brain tissue was emersed in 10% formaldehyde for more than 24 h, and then embedded in paraffin, sectioned and stained with the Nissl method. Stained sections (corresponding to coronal slices from the rostral region (Bregma +1.24mm to −4.16 mm)) were photographed and the most severely damaged brain sections were selected for display (Bregma −2.26 ± 0.20 mm). Sections were analyzed by Image J software to count the cells that tested positive for Nissl (clear Nissl bodies and nuclei) in both sides of the cortex and striatum. The reasons for choosing these two specific areas (cortex and striatum) for analysis were as follows: firstly, we measured these two areas during temperature measurement, so the neuron damage analysis also corresponded to these two areas; secondly, the neurofunctional assessment of the present research mainly focused on sensory and motor function, which were the main responsibility of these two areas. On each side of the cortex and striatum, five regions were randomly selected. The selected region of interest is completely symmetrical on both hemispheres. The ratio of Nissl-positive cells in the ipsilateral hemisphere to the contralateral hemisphere was calculated. A lower Nissl body ratio indicated more serious neuron damage.

## Evans blue leakage

Evans blue leakage measurement was performed according to the previously reported method [28, 35]. The tail vein was punctured with a 2% Evans blue dye solution (wt/vol in PBS, 3 mL/kg, 0.84-0.96 ml due to the weight of rats ranging from 280 to 320 g, Solarbio Bioscience & Technology Co., LTD, China), and rats were killed 2 h later through cardiac perfusion with saline. The brains were then removed and photographed to visualize Evans Blue leakage. Subsequently, ischemic half-brain tissue was homogenized in one milliliter of formamide solution (Solarbio Bioscience & Technology Co., LTD, China) to create a cell suspension. After a 24-h incubation period at 60°C, the material was centrifuged for 10 min at 5000 rpm. The Evans blue content was calculated from a standard curve constructed by

optical density readings of the supernatant at 635 nm using a microplate spectrophotometer (Bio-Tek, USA).

## Brain water

Fresh brain tissue was weighed to calculate the wet weight, which was then dried in an oven to obtain dry weight. Brain tissue water content percentage was calculated as (wet weight - dry weight) / wet weight × 100% [36].

## Cerebral blood flow

The relative CBF quantify was measured using a Laser speckle imaging (LSI, RWD Science Co., LTD China) following a previously published technique [37]. The rats were placed on a prone position and their heads were fastened in a stereotaxic device after shaving and iodophor disinfection. A longitudinal incision was made in the skin over the cranium. The cranium, from bregma to lambda, was thinned using a dental drill under a dissecting microscope until CBF could be clearly quantified by LSI. The mean CBF of both sides was calculated and the operation ipsilateral side's CBF was expressed as a percentage of the value on the contralateral side.

## Immunofluorescence

The immunofluorescence labeling procedure was conducted as previously described [38]. Briefly, the coronal brain slices (20 µm thickness) and seeded cells were incubated with the blocking solution (10% secondary antibody species serum and Triton 0.05-0.1% in PBS) for 1 h. The sections and cells were incubated overnight at 4°C with the corresponding primary antibodies diluted in the blocking solution. Sufficient secondary antibodies conjugated to fluorophores were utilized. The pericytes were also incubated with phalloidin and DAPI (Solarbio Bioscience & Technology Co., LTD, China) to visualize F-actin and cell nucleus. Finally, fluorescent images were recorded for subsequent analysis. The primary antibodies included anti-Rat CD31 (Cat#GB120005, Servicebio, China), anti-Rat Ly6G (Cat#GTX40912, GeneTex, USA), anti-Mouse ZO-1 (Cat#33-9100, Invitrogen, USA), anti-Rat α-SMA (Cat#14395-1-AP, Proteintech, USA) and anti-Rat TRPM8 (Cat#ACC-049, Alomone Labs, Israel).

## OGD/R model

Neural cells (HT22), cerebral microvessel ECs (bEnd.3) and rat cerebral primary pericytes were washed and cultured in glucose-free Dulbecco's modified Eagle's medium (DMEM, Gibco, USA) without fetal bovine serum (FBS), and subsequently moved into an anaerobic chamber containing 5% $CO_2$ and 95% $N_2$ for 4-hour incubation. The cells were then divided into 4 groups: OGD/R group, the cells were placed back into the normoxic incubator (37°C, 5% $CO_2$) with regular media containing 10% FBS (Gibco, USA) for 24 h; OGD/R+HT group, the cells were placed in a hypothermia normoxic incubator (32°C) with regular media; OGD/R+MgSO$_4$ and OGD/R+MgSO$_4$+HT group were placed in 37°C and 32°C normoxic incubator, respectively, with regular media containing 10 mM MgSO$_4$. A 10 mM concentration of MgSO$_4$ was selected based on findings indicating its optimal neuroprotective efficacy against OGD/R-induced neuronal injury (Figure S2). Cells in the control group were cultured under normal conditions in the absence of OGD/R or other treatments for 28 h.

## Primary pericyte culture

The SD rats were euthanized through vertebrae removal, and immersed in a 75% ethanol beaker for disinfection. The brain was removed and the cerebral cortex tissue was separated and cut into 1 mm$^3$ fragments. It was washed with PBS once and placed in a centrifuge tube. Subsequently, a digestion solution (collagenase II) was added for incubation at 37°C in water bath on a shaker for 1 h. The tissue suspension was centrifuged at 800 g for 5 min and resuspended to precipitate with 20% bovine serum albumin. This was followed by a further centrifugation at 1200 g for 25 min and incubation with digestive solution (dispase II) to digest at 37°C for 40 min. The solution was centrifuged at 800 g for 5 min. The precipitate was resuspended in PBS and slowly added to the upper layer of a 35% Percoll continuous density gradient cell separation solution (obtained by centrifugation at 12000 g for 1 h). The solution was then centrifuged at 1000 g for 10 min, and the yellow-white layer (microvessel) near the bottom of the red precipitate was extracted.

The microvascular segment was centrifuged at 800 g for 5 min. The cells were resuspended in a complete culture medium of rat brain microvascular pericytes, implanted into culture dishes pre-coated with polylysine, and incubated in an incubator with a constant temperature at 37°C and 5% $CO_2$ for 48 h. The purity of the cells was identified by α-SMA (Figure S3).

## Normal pericyte experiment

The pericytes were divided into two groups: the MgSO$_4$ group and control group. Cells in the MgSO$_4$ group were treated in a medium containing 10 mM MgSO$_4$. Those in the MgSO$_4$ and control groups were incubated in a normoxic incubator at 32°C for 24 h, and then rewarmed to 37°C. The MgSO$_4$ was added to the cells just before they were transferred to the

incubator.

The pericytes were also incubated with the TRPM8 antagonist and agonist. For the antagonist tests, the pericytes were treated with 10 µM AMTB [39], and incubated in a normoxic incubator at 32°C for 24 h. The pericytes incubated without AMTB treatment served as the control. AMTB was applied just before the cells were transferred to the incubator. For the agonist tests, the pericytes were incubated with 10 mM $MgSO_4$ and 0.1mM menthol in a normoxic incubator at 37°C [40]. Pericytes incubated in the absence of $MgSO_4$ served as the control.

### Cell viability

Cell viability was assessed using the cell counting kit-8 (CCK-8) assay and by measuring lactic dehydrogenase (LDH) release concentration. Cells were seeded at a density of 5000 cells/well in 96-well plates. For the CCK-8 assay, 10 µL of CCK-8 solution (Beyotime, China) was added to each well and incubated at 37°C for 1 h, followed by absorbance measurement at 450 nm. For LDH release measurement, a commercial LDH assay kit (Beyotime, China) was used. Briefly, supernatants collected from each well were transferred to a new 96-well plates and incubated with the reagent of assay kit at room temperature (RT) for 30 min. Finally, the absorbance was measured at 490 nm.

### Intracellular $Ca^{2+}$ detection

Intracellular $Ca^{2+}$ imaging and quantification was conducted using a Fluo-4 $Ca^{2+}$ detection kit (Beyotime, China). Cells were incubated with Fluo-4 staining solution at 37°C for 30 min and continuously observed and photographed with a fluorescence microscope. The intracellular calcium ion concentration was calculated based on the fluorescence intensity using the Image J software.

### Intracellular reactive oxygen species detection

Cells were treated with 10 µM DCFH-DA (Beyotime, China) in a serum-free medium for 20 min and washed thrice. Subsequently, the fluorescence of DCF at 488/525 nm was measured using a fluorescence microplate reader (Bio-Tek, USA) to determine the concentration of ROS.

### Assessment of cell apoptosis rate

After trypsinization, adherent cells were collected and washed twice. They were then resuspended in 1× Binding Buffer and 100 µL of the suspension was added to the tube. It was then mixed with 5 µL of Annexin V-FITC and mixed gently. 10 µL of propyl iodide (PI) dye was added and suspension was mixed again and allowed to incubate at RT for 20 min. Annexin V-positive and PI-negative cells indicated early apoptotic cells, while both Annexin V-positive and PI-positive cells represented late apoptotic cells.

### Cell contraction assay

A collagen gel-based cell contraction assay kit (CBA-201, Cell Biolabs, USA) was utilized to compare the contraction function of primary pericytes. Briefly, the pericytes were resuspended in pericytes growth medium. The cells were mixed with a collagen gel working solution on ice. Next, collagen polymerization was induced by incubating the cell-gel combination solution (0.5 mL, containing $2 \times 10^5$ cells) in a 24-well plate for 1 h at 37°C. Subsequently, the cells were treated according to the previously described groupings to assess contractile force. Each gel was continually photographed and quantified using Image J software. Cell contraction (%) is equal to (well area – gel area) / well area × 100%.

### Statistical analysis

The data were analyzed with SPSS 17.0, and expressed as mean ± standard deviation for continuous variable and as percentages (%) for categorical variable. Differences between groups were compared using the one-way ANOVA and nonparametric tests.

## Results

### IA-SCMI decreased the brain temperature

To compare the neuroprotective effect of IA-SCMI and IA-SCSI, we evaluated the cooling effect of IA-SCMI after MCAO. During the infusion, IA-SCMI gradually reduced the temperature of ipsilateral cerebral striatum and cortex to about 32°C, which was significantly lower than that of the contralateral side, and slowly warmed up after infusion. Moreover, the core temperature (rectal temperature) remained nearly unchanged (Figure 1B). The cooling effect of IA-SCMI on the ipsilateral brain was comparable to that of IA-SCSI (Figure S4A), and neither IA-SMI nor IA-SSI induced significant hypothermic effects (Figure S4B). Moreover, IA-SI including IA-SCMI did not impact vital signs, as there were no differences in MABP, heart rate, $pO_2$ and $pCO_2$ (Figure S5).

### IA-SCMI improved functional recovery

Having demonstrated the cooling effect of IA-SCMI, we compared the neurological behavioral protective effects between different treated groups. Following MCAO, the mNSS score and the time taken

for the rats to touch and remove the tap significantly increased, and the time taken to fall off the rotating rod was shortened. Although the neural function of the MCAO group rats partially recovered after 14 days, residual neurological deficiency was still detected (Figure 1C-F). IA-SSI did not alter neurological function following MCAO (Figure 1C-F). However, based on the results of mNSS and the time taken to touch the tape, IA-SMI partially alleviated the neurological impairment (Figure 1C-E). IA-SCSI treatment significantly improved neurological function compared to MCAO, IA-SSI and IA-SMI (Figure 1C-F). Moreover, IA-SCMI further promoted the recovery of neural function (Figure 1C-F). Although no statistically significant differences were observed, IA-SMI appeared to reduce mortality compared to the MCAO and MCAO+IA-SSI groups. IA-SCSI seemed to further lower mortality, with the IA-SCMI group exhibiting the lowest mortality rate (Figure S6).

### IA-SCMI protected brain integrity

Considering the satisfactory protective effects on the neurological behavior of IA-SCMI, *ex vivo* brain integrity of neuron and BBB was further investigated. The results indicated that IA-SCSI decreased the infarction volume compared to MCAO, MCAO+IA-SSI and MCAO+IA-SMI groups. Moreover, IA-SCMI exerted a stronger protective effect than IA-SCSI (Figure 2A-B). The Evans blue leakage and brain water content test results showed a similar trend, demonstrating that IA-SCMI had the best BBB-protective effects (Figure 2E-G). Interestingly, quantitative analysis of Nissl bodies in nerve cells on the seventh day (Figure 2C-D) found that IA-SCSI and IA-SCMI conferred protection on cortical nerve cells compared to MCAO, MCAO+IA-SSI and MCAO+IA-SMI, with IA-SCMI performing relatively better compared to IA-SCSI, but the difference was not significant. Compared to MCAO and MCAO+IA-SSI, MCAO+IA-SMI showed higher protective effects on striatal neurons, with IA-SCSI having better protective effects than IA-SMI. Overall, IA-SCMI yielded the best protective effects. In summary, these results indicate that IA-SCMI can efficiently prevent brain integrity damage to the greatest extent.

### IA-SCMI enhanced CBF

Given the limited research on the impact of IA-SCSI on CBF, we initially conducted our study in normal rats. Following immediate infusion, both IA-SCSI and IA-SMI had no effect on CBF. However, IA-SCSI reduced the ipsilateral CBF, while IA-SCMI inhibited this trend (Figure 3A). Following infusion, CBF exhibited gradual recovery pattern (Figure S7), possibly due to brain temperature rewarming. Considering the transient CBF effects of IA-SI on normal rats, we further investigated the effects in MCAO rats. Figure 3B and Figure S8 show that MCAO significantly reduced ipsilateral CBF, and immediately after infusion, IA-SMI restored the CBF more effectively compared with IA-SSI, and this effect lasted up to 24 h later (not significant). However, compared to IA-SSI and IA-SMI, IA-SCSI decreased CBF immediately, and 24 h later, the CBF of the IA-SCSI group was still slightly lower than that of the IA-SSI group (not significant) and much lower than that of the IA-SMI group. Interestingly, although the CBF of IA-SCMI was lower compared with that of IA-SSI and IA-SMI immediately after infusion, it was higher than that of IA-SCSI. Further analysis revealed that CBF in IA-SCMI group was the highest among all groups 24 h after infusion. We hypothesized that the underlying reason for this phenomenon might be the delayed relaxation of microvessels during reperfusion due to hypothermia, leading to thrombus accumulation. Despite the eventual recovery of brain temperature and the long-term protective effect of hypothermia on ischemia-reperfusion injury, the early microvessel contraction and microthrombosis were irreversible, resulting in a permanent reduction in cerebral blood flow. Magnesium ions can reduce the immediate effect of hypothermia on CBF, and combined the protective effect with hypothermia late, thereby inhibit vessel contraction and microthrombosis leading to CBF enhancement. Based on this hypothesis and previous evidence that neutrophils are the main cells that block microvessels after MCAO recanalization [38], we further measured the content of neutrophils in capillaries and found that the number of neutrophils blocking in capillaries in group IA-SCSI was comparable to that of the group IA-SSI, while IA-SMI treatment significantly reduced the number of neutrophils and IA-SCMI exhibited the best inhibitory effect on neutrophil blockage (Figure 3C).

### Hypothermia combined with MgSO$_4$ protected neurons and ECs *in vitro*

Considering the excellent *in vivo* neuroprotective and BBB protective effects, we further investigated the synergistic effects of hypothermia and MgSO$_4$ *in vitro*, which was conducted in neuron first (Figure 4A). The CCK-8 assay showed that the cell viability decreased after OGD/R injury, and both hypothermia alone and MgSO$_4$ alone could reverse this effect. Furthermore, the combination of hypothermia and MgSO4 demonstrated the most beneficial effect on preserving cell viability (Figure 4B). This trend was also

confirmed by the LDH release assay (Figure S9A). $Ca^{2+}$ overload and ROS production were two of the most common damaging factors for cells following OGD/R treatment. $Ca^{2+}$ regulation may be a potential mechanism underlying the effectiveness of the combination therapy. Thus, we measured the cellular concentration of $Ca^{2+}$ and ROS. It was observed that OGD/R increased $Ca^{2+}$ and ROS in neuron and both $MgSO_4$ alone and hypothermia alone could revers $Ca^{2+}$ change. However, hypothermia alone reduced a larger concentration of ROS than $MgSO_4$ alone.

Furthermore, the combination of hypothermia and $MgSO_4$ exhibited the most significant effect in reducing both $Ca^{2+}$ and ROS (Figure 4C-E). To further elucidate the impact on cell viability, apoptosis was measured, as it is a critical factor contributing to cell death. The results indicated that the combination therapy could most effectively prevent cell apoptosis, and both hypothermia alone and $MgSO_4$ alone were equally effective in reducing neural apoptosis. (Figure 4F-G).
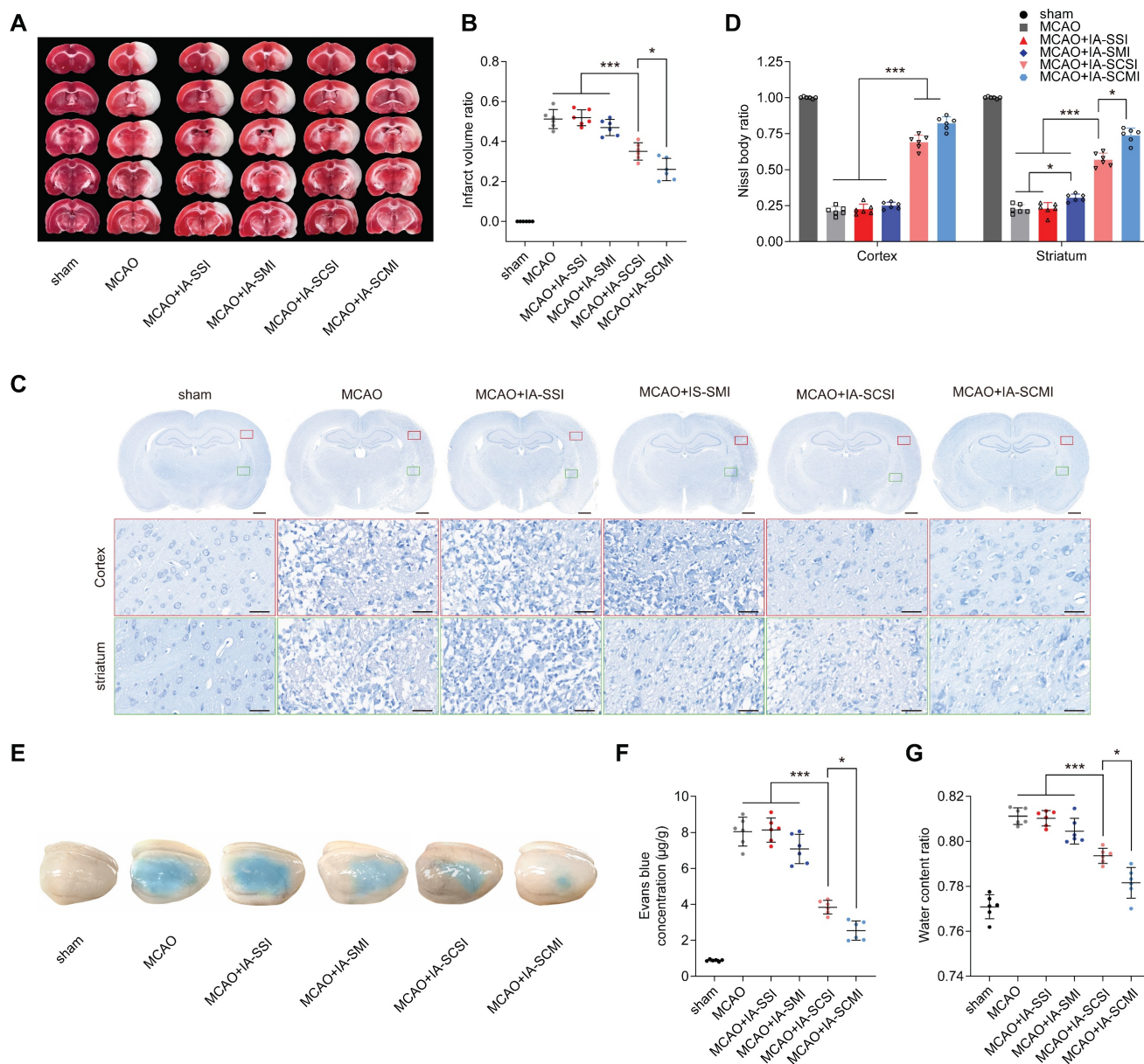


**Figure 2.** The protective effects of IA-SCMI on brain integrity. (A-B) Representative images of brain slices stained with TTC and summary data of relative infarction volumes. (C-D) Representative images of Nissl stained brain slices and summary data of relative Nissl body number. Scale bars: 1 mm and 25 μm. (E-F) Representative images of brain tissue penetrated by Evans blue and summary data of relative Evans blue content. (G) The relative water content of ipsilateral brain tissue. n=6 for each group. * $p < 0.05$, *** $p < 0.001$.
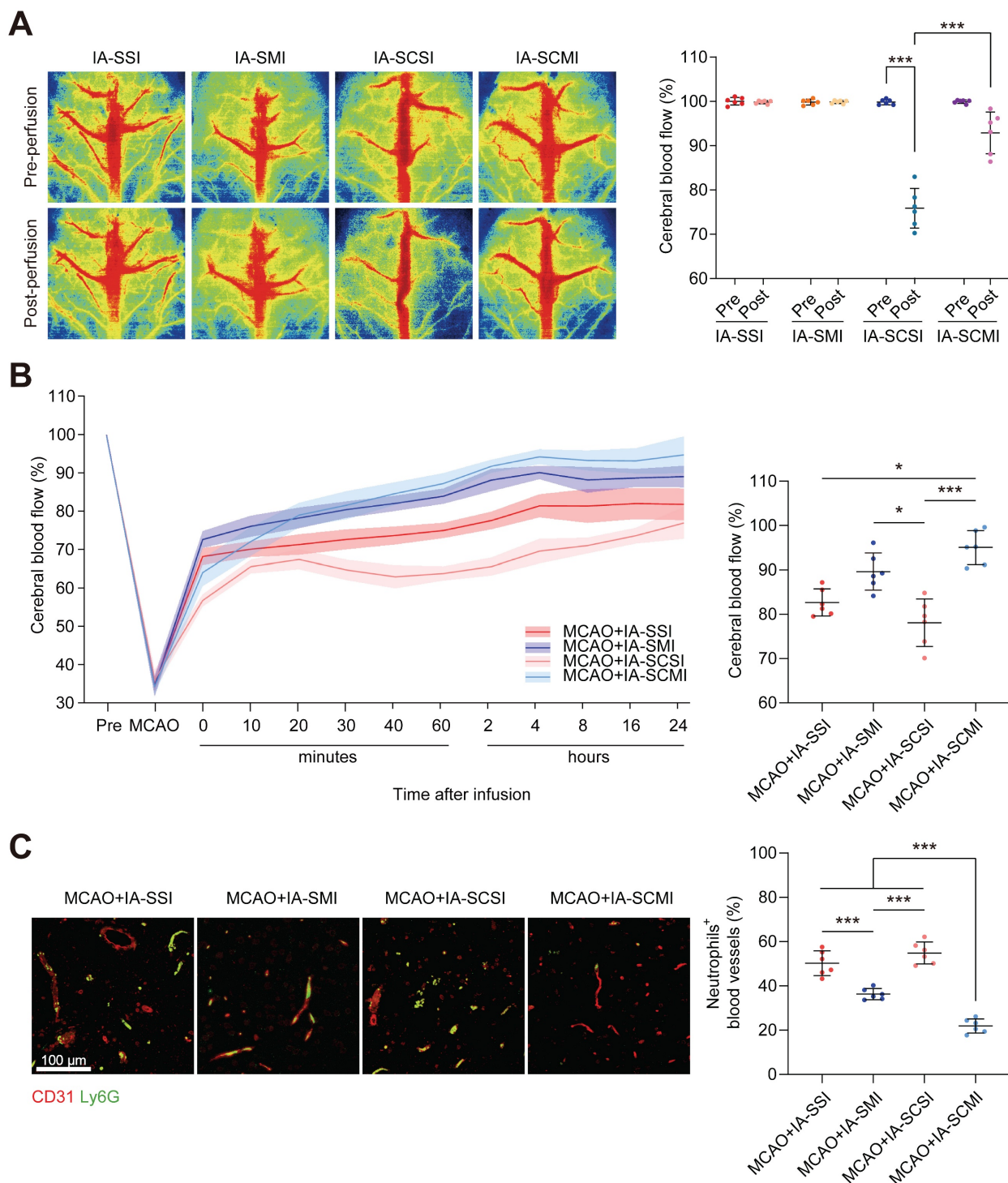
**Figure 3.** The CBF protection effect of IA-SCMI. (A) LSI image of CBF immediately after IA-SI in normal rats and summary data of related CBF. (B) Temporal profile of CBF in MCAO rats with IA-SI and summary data of the related CBF at the 24-h time point after IA-SI. (C) Fluorescence images of entrapped neutrophils (Ly6G, green) in capillaries (CD31, red) and quantification. n=6 for each group. * $p < 0.05$, *** $p < 0.001$.

Subsequently, we investigated the combined effect of hypothermia and $MgSO_4$ on microvessel ECs, an important component of BBB (Figure 5A). From the perspective of cell viability, LDH release concentration and intracellular $Ca^{2+}$ and ROS, hypothermia combined with $MgSO_4$ exhibited the best protective effect on ECs after OGD/R injury and

hypothermia alone ranks second, with $MgSO_4$ alone ranking last (Figure 5B-E and Figure S9B). The expression level of tight junction proteins in endothelial cells serves as a crucial marker of cell barrier function. Therefore, the expression level of ZO-1, one of the tight junction proteins, was quantified. The results indicated that OGD/R injury

significantly downregulated ZO-1 expression in ECs, and MgSO$_4$ alone only partially rescued ZO-1 expression. Moreover, hypothermia alone had a better salvage effect on ZO-1 reduction, whereas hypothermia combined with MgSO$_4$ had the highest inhibitory effect (Figure 5F-G). These results indicated hypothermia combined with MgSO$_4$ could simultaneously protect neurons and EC cells, consistent with *in vivo* data.
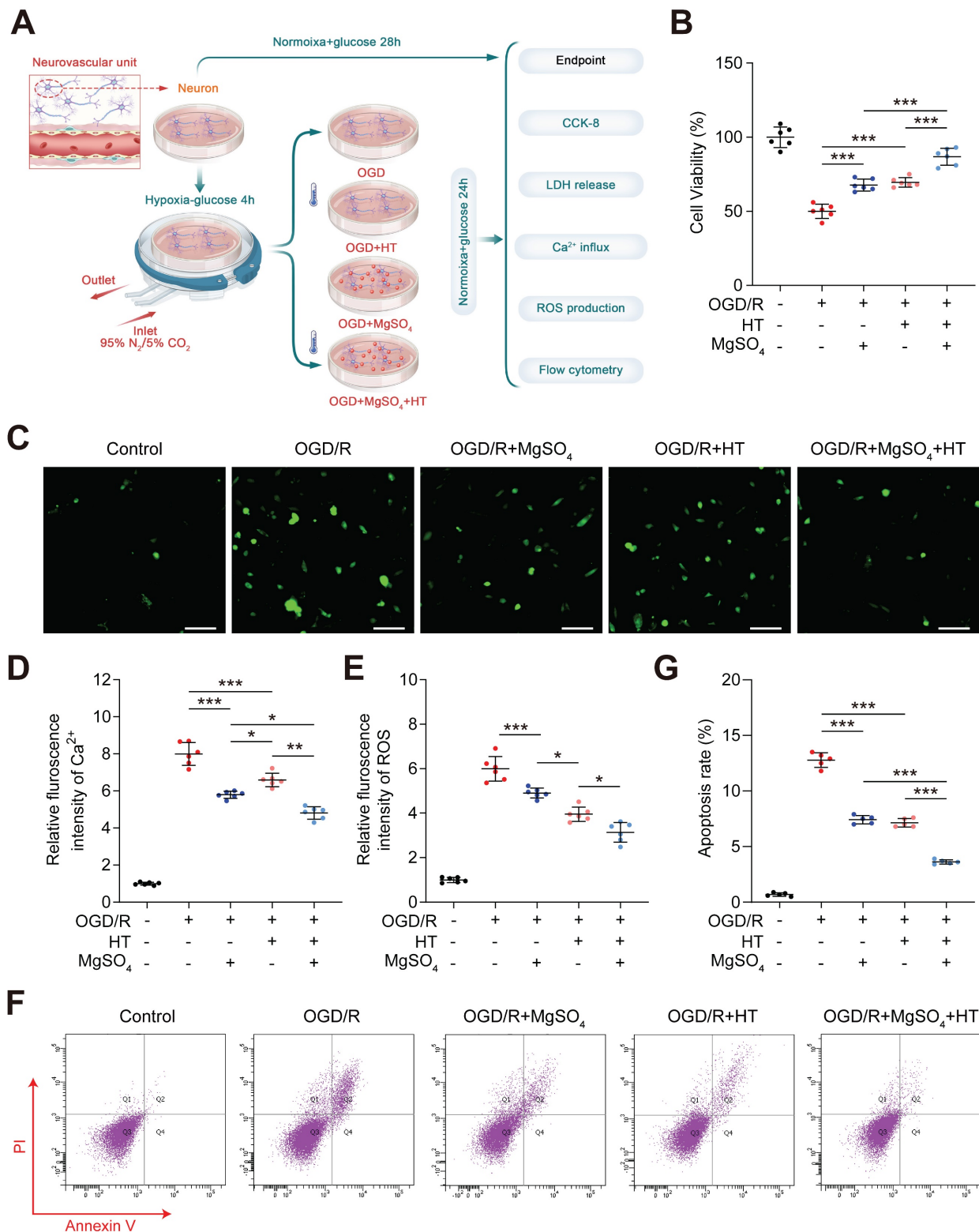


**Figure 4.** *In vitro* effects of the combination hypothermia and MgSO$_4$ on neurons. (A) The flow chart of neural cell experiments. (B) Cell viability assay (n=6). (C-D) Fluorescence imaging of intracellular Ca$^{2+}$ and summary data of relative fulroscence intensity of Ca$^{2+}$ in neuron (n=6). scale bars: 20 μm. (E) Summary data of relative fulroscence intensity of ROS in neuron (n=6). (F-G) Flow cytometry and quantification of cell apoptosis rate (n=5). * $p < 0.05$, ** $p < 0.01$, *** $p < 0.001$.
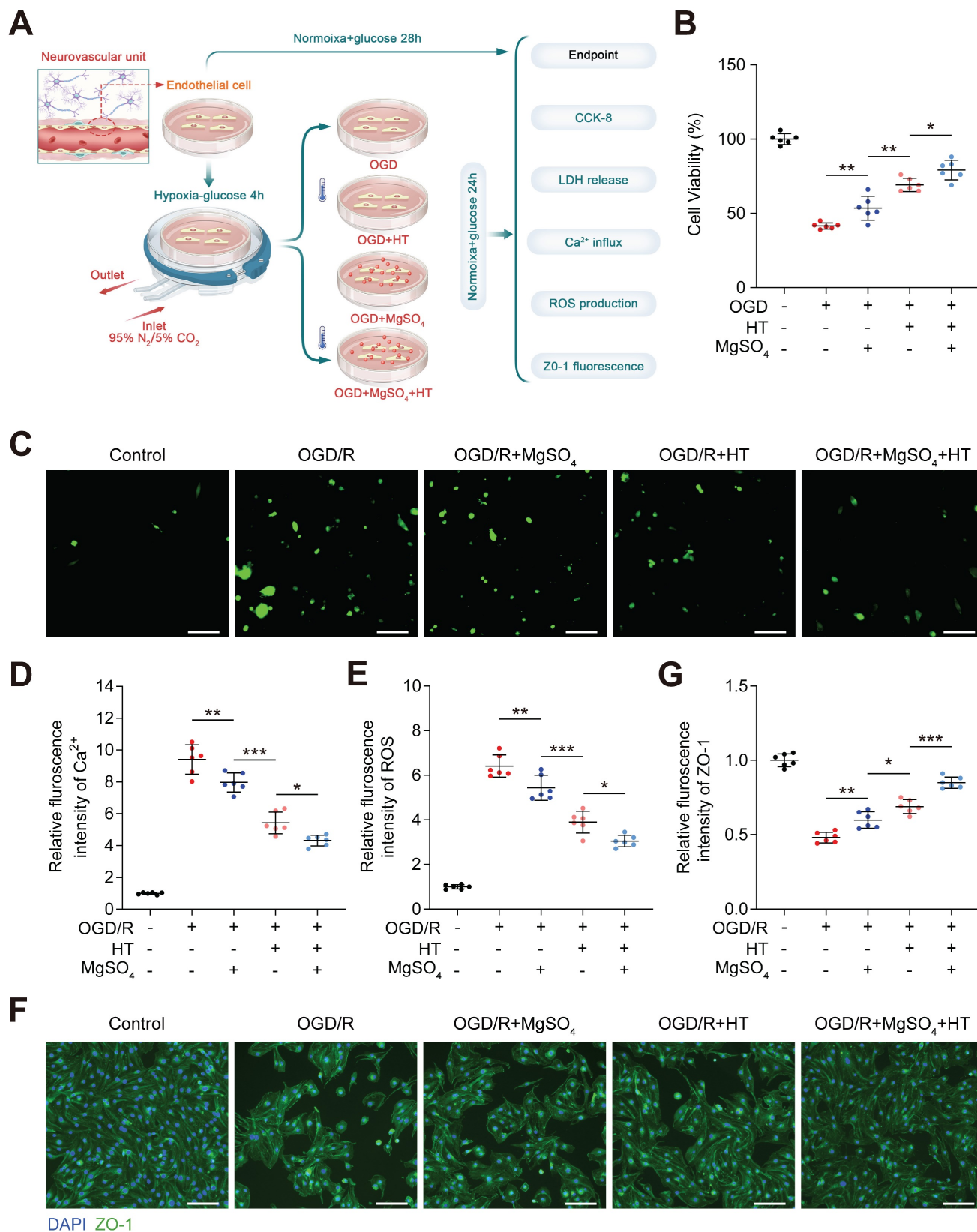
**Figure 5.** *In vitro* effects of the combination of hypothermia and MgSO₄ on microvessel EC. (A) The flow chart of microvessel EC experiments. (B) Cell viability assay. (C-D) Fluorescence imaging of intracellular $Ca^{2+}$ and summary data of relative fluorescence intensity of $Ca^{2+}$ in ECs. Scale bars: 20 µm. (E) Summary data of relative fluorescence intensity of ROS in ECs. (F-G) Fluorescence imaging and quantification of cellular ZO-1 expression. n=6 for each group. * $p < 0.05$, ** $p < 0.01$, *** $p < 0.001$.

## MgSO₄ counteracted the early harmful effects of hypothermia on pericytes *in vitro* to exert a synergistic role late

Previous studies have demonstrated that pericytes could control CBF [41]. Therefore, we examined the effects of MgSO₄ alone, hypothermia alone, and the combination of the two on pericytes *in vitro* (Figure 6A). Pericyte death has been linked to long-term capillary contraction, and therefore, we explored the survival rate of pericytes [41]. Hypothermia alone did not alter the cell viability and LDH release following OGD/R injury. However, MgSO₄ alone rescued pericyte death, and hypothermia combined with MgSO₄ had a better protective effect (Figure 6B and Figure S9C). Next, we investigated pericyte contraction rate by examining the reduction of gel area. After OGD injury, pericyte exhibited partial contraction, and after reoxygenation, pericyte contraction increased over time up to 24 h. Moreover, exposure to hypothermia alone exacerbated the early contraction, but the final contraction rate of OGD/R+HT group was comparable with the rate of the OGD/R group. However, treatment with MgSO₄ alone decreased early contraction and this effect lasted up to 24 h. Interestingly, the combined treatment group could counteract the early contraction-promoting effect of hypothermia alone, meanwhile, compared with the control group, there is even some protective effect. Moreover, the combination therapy yielded the highest inhibitory effect on contraction of pericytes (Figure 6C). Since Ca²⁺ influx and overload are important factors that induce pericyte death and contraction, we measured the intracellular Ca²⁺ concentration. The pattern of intracellular calcium ion increase closely resembles the pattern of pericyte contraction degree increase, except for a lack of difference in intracellular Ca²⁺ levels between the combination therapy group and the OGD/R group 30 min after reoxygenation (Figure 6D-E). Based on these results, we speculated that hypothermia alone might induce early Ca²⁺ influx into pericyte after OGD/R to cause intense premature contraction and death of pericytes, which will offset the late-stage inhibitory effect of hypothermia on Ca²⁺ influx. However, MgSO₄ alone persistently inhibited Ca²⁺ influx to suppress the contraction and death of pericytes. Moreover, after combination therapy, MgSO₄ abolished the early harmful effects of hypothermia on pericytes. Notably, combination therapy played a synergistic protective role in the later stages, thus achieving the best protective effect.

The mechanism of premature influx of Ca²⁺ into pericytes caused by hypothermia was further investigated in normal pericytes. Hypothermia stimulated normal pericyte contraction due to Ca²⁺ influx, while Mg²⁺, as a natural antagonist of Ca²⁺, inhibited this phenomenon (Figure S10). The *in vitro* and *in vivo* results indicated that the contraction effect of hypothermia and Mg²⁺ on pericytes maybe an inherent phenomenon that is not affected by I/R and OGD/R injury. Previous studies have reported that TRPM8, a cold-sensitive channel, is expressed on smooth muscle cells of cerebral blood vessels from piglets. TRPM8 regulates Ca²⁺ influx into cells by sensing cold stimuli [42]. Therefore, TRPM8 may mediate the aforementioned effects. Given that TRPM8 has not been reported in cerebral pericytes of rats, its expression was explored in this study, and the effects of hypothermia and MgSO₄ on TRPM8 were also investigated. Cellular immunofluorescence showed that TRPM8 was expressed on rat cerebral pericytes (Figure S11). The effects of hypothermia and TRPM8 agonist, menthol, on the contraction and Ca²⁺ influx of pericytes were inhibited by the TRPM8 antagonist, AMTB, and MgSO₄, respectively (Figure S12). These findings suggest that the early Ca²⁺ influx effect of mild hypothermia on pericytes is mediated by the activation of the TRPM8 channel, while MgSO₄ can antagonize this channel, thereby inhibiting the effects of hypothermia.

## Discussion

This study explored the possibility of MgSO₄ as a novel hypothermia infusion solution for treating AIS. The result showed that IA-SCMI selectively cooled infarction ipsilateral brain tissue, and compared to IA-SCSI and IA-SMI, IA-SCMI more efficiently reduced neurological deficits. Moreover, IA-SCMI improved neuron viability and BBB integrity. In contrast, IA-SCSI had no beneficial effects on CBF, but IA-SCMI abolished the early CBF reduction induced by hypothermia and improved CBF recovery. Furthermore, the combination of hypothermia and Mg²⁺ protected neurons and cerebral microvessel ECs by inhibiting Ca²⁺ influx *in vitro*. *In vitro* pericyte experiments revealed that hypothermia had no protective effect on pericyte survival and promoted early rapid contraction through the activation of TRPM8. In contrast, combination therapy could counteract the early detrimental effects of hypothermia and synergistically inhibited Ca²⁺ influx into pericytes, promoting their viability and inhibiting their contraction (Figure 7).
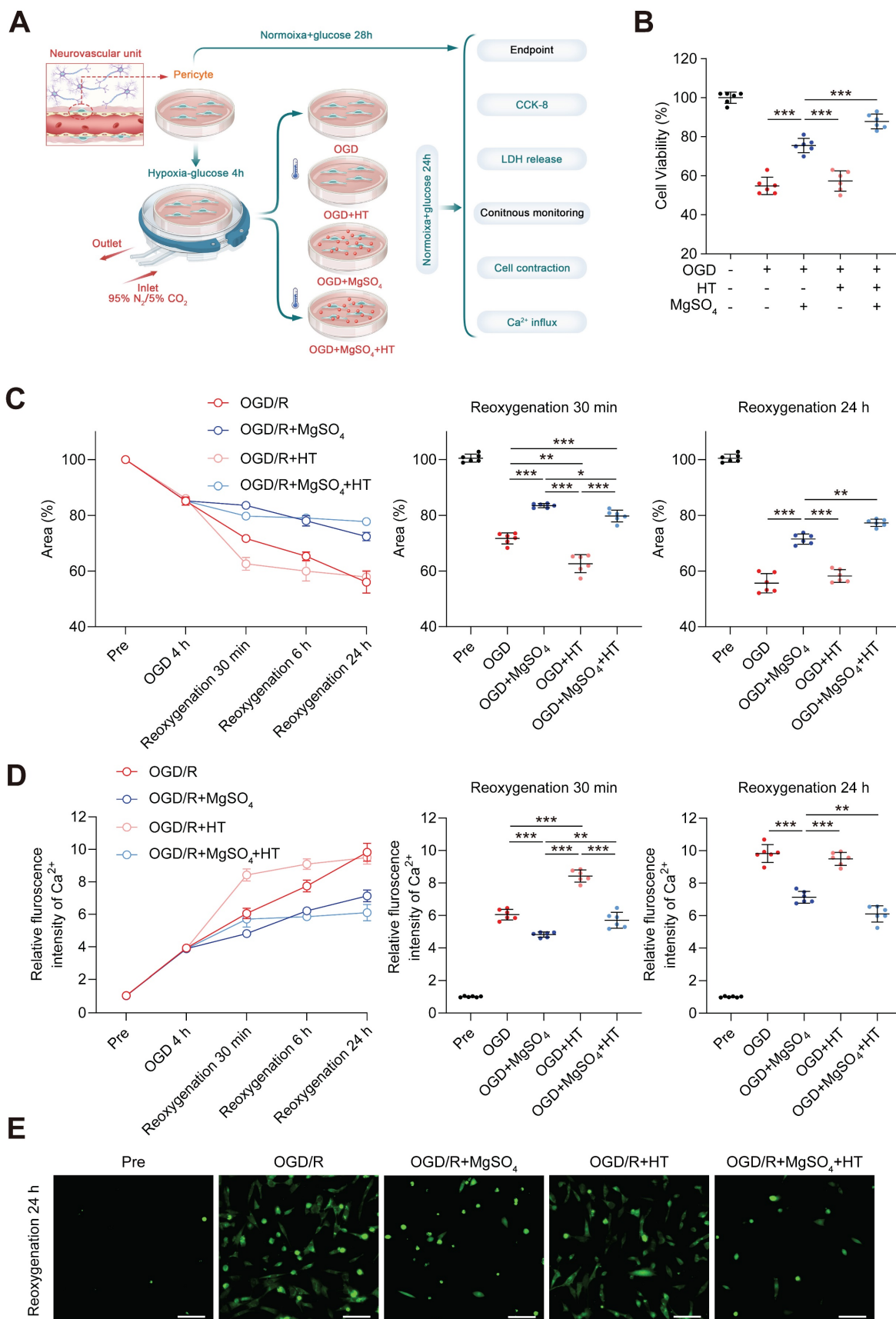
**Figure 6.** *In vitro* effects of the combination of hypothermia and MgSO₄ on pericytes. (A) The flow chart of pericyte experiments. (B) Cell viability assay. (C) Quantitative analysis of the area of collagen gel. (D) Quantitative analysis of relative fluorescence intensity of Ca²⁺ in pericytes. (E) Fluorescence imaging of intracellular Ca²⁺ after reoxygenation 24 h. scale bars: 20 µm. n=6 for each group. * $p < 0.05$, ** $p < 0.01$, *** $p < 0.001$.
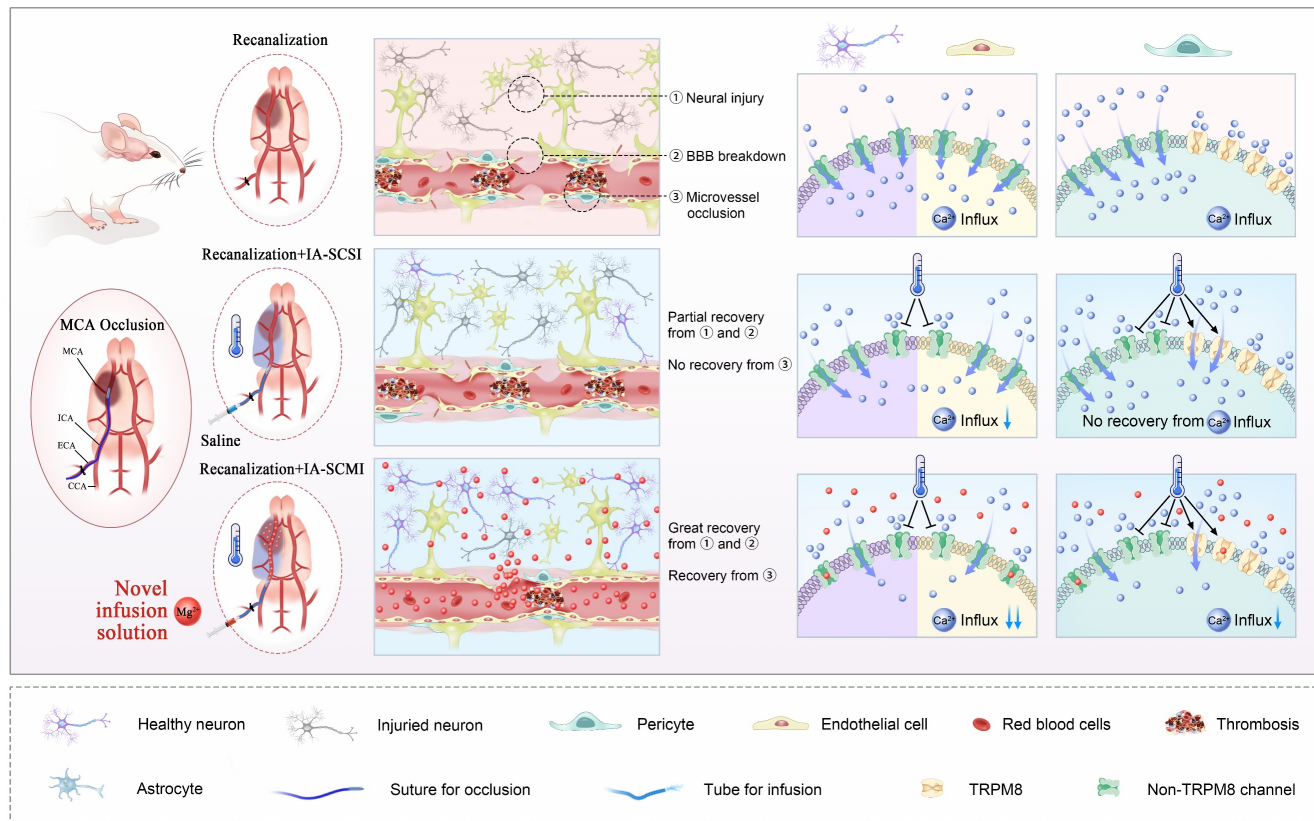
**Figure 7.** MgSO₄ as a novel hypothermia infusion solution for promoting AIS recovery by regulating $Ca^{2+}$ in NVUs. After I/R injury, the infarction region undergoes severe neural injury, BBB breakdown and microvessel occlusion, which were triggered by $Ca^{2+}$ influx into neurons, cerebral microvessel ECs and pericytes. IA-SCSI cooled the brain and promoted partial recovery from neural injury and BBB breakdown but could not rescue microvessel occlusion. *In vitro* cell experiments confirmed that hypothermia could partially inhibit $Ca^{2+}$ influx into neurons and cerebral microvessel ECs but did not affect the total amount of calcium ions in pericytes because hypothermia increased $Ca^{2+}$ influx through TRPM8. Moreover, IA-SCMI demonstrated significant recovery from neural injury and BBB breakdown, and enhanced microvessel circulation. The combination of hypothermia and $Mg^{2+}$ exerted stronger inhibitory effects on $Ca^{2+}$ influx compared with hypothermia alone in NVU cells. MCA, middle cerebral artery; ICA, internal carotid artery; ECA, external carotid artery; CCA, common carotid artery; IA-SCSI, intra-artery selective cooling saline infusion; IA-SCMI, intra-artery selective cooling MgSO₄ infusion; BBB, brain-blood barrier.

## Innovation points of IA-SCMI

Compared to the existing simple hypothermia therapies for AIS, such as whole-body cooling, ice cap cooling, and IA-SCSI, IA-SCMI encompasses the effects of targeted brain hypothermia and targeted drug therapy through arterial infusion pathway. In the present study, we found that IA-SCMI achieved superior therapeutic effects compared to IA-SCSI. Therefore, the innovative findings of our research indicate that monotherapy may not be sufficiently effective for AIS. Instead, AIS should be treated with a combination of targeted physical (hypothermia) and pharmacological (MgSO₄) therapies, akin to the approach used in some cancer treatments (e.g., targeted radiotherapy plus chemotherapy), in order to achieve the best possible outcomes. This innovation points also provides ideas for future IA-SI research, which can use cooling solutions containing different neuroprotective drugs as infusion media to better treat AIS. Another innovation of this study is the exploitation of the $Ca^{2+}$ antagonistic effect of MgSO₄ to potentiate the protective effects of hypothermia on neuron and ECs, and reverses the adverse effects on CBF. Future studies should leverage this novel mechanism to select drugs that can achieve synergistic therapy based on hypothermia.

## Hypothermia combined with $Mg^{2+}$ for treating AIS

The combination of hypothermia and $Mg^{2+}$ has shown potential to treat AIS in many previous studies. For example, both Zausinger *et al.* [16] and Campbell *et al.* [17] have found that the combination of intravenous administration of $Mg^{2+}$ and surface cooling is more effective in treating AIS than either treatment alone. Their results strongly support the findings of the present research. Moreover, intraarterial infusion $Mg^{2+}$ into infarction region can amplify the neuroprotective effect than intravenous infusion [43], and compare to surface cooling, IA-SCI has faster and stronger cooling effect [10]. Therefore, IA-SCMI has great potential to achieve excellent therapeutic effects and our results confirmed this potential.

## Hypothermia combined with Mg²⁺ for treating other cerebral infarction disease

Besides AIS, several other cerebral infarction diseases such as hypoxic-ischemic encephalopathy in newborns and cardiac arrest, have been studied to examine whether they can benefit from combination therapy of hypothermia and Mg²⁺. For instance, Zhu *et al.* found that combined therapy was more effective at reducing CA1 neuronal death than either treatment used alone in global cerebral ischemic rats [44]. In clinical practice, hypothermia is the only effective treatment for patients with neonatal hypoxic-ischemic encephalopathy and the combination of hypothermia and MgSO₄ has also been widely tested in clinical practice. Rahman *et al.* conducted a pilot study to primarily validate the safety of combination therapy [45]. These results provide indirect support for the efficiency and safety of combination therapy.

## The combined protective effects of hypothermia and Mg²⁺ on nerves and BBB

Numerous studies have demonstrated the protective effect of hypothermia on neural injury and BBB breakdown [46, 47]. Similarly, Mg²⁺ was reported to attenuate neural death and BBB damage [48, 49]. Therefore, the combined application of hypothermia and Mg²⁺ may have synergistic protective effects on nerves and BBB. Although this combination therapy decreased the infarct size and promote neurological recovery, it is not known whether it can improve the integrity of BBB, and the protective mechanism first discovered in this study has not been thoroughly explored. Magnesium ions, as a naturally powerful Ca²⁺ antagonist, could conquer Ca²⁺ overload [19]. Moreover, hypothermia plays a multiple role in Ca²⁺ influx, such as through inhibiting oxidative stress damage and stabilizing mitochondrial function [50]. Thus, Ca²⁺ regulation seem to be the potential mechanism for combination therapy. The hypothesis was confirmed through *in vitro* experiments. Although the effects of hypothermia alone and Mg²⁺ alone on Ca²⁺ influx in neurons and ECs varied, the combination of these two exhibited the best protective effect in both types of cells. Moreover, studies have shown that combination therapy more efficiently inhibit ROS and cell death. Therefore, such a combination will inhibit neuronal apoptosis and loss of tight junction proteins in ECs.

## The combined regulation effects of hypothermia and Mg²⁺ on CBF

Temperature influences the blood flow is a common phenomenon in whole body and previous research has demonstrated that CBF can also be modulated by focal temperature [15]. This result aligns with our findings, suggesting that CBF can be stably suppressed under hypothermic conditions. This phenomenon partially explains why CBF may not fully recover after reperfusion following hypothermia. However, Mg²⁺ can counteract this early adverse effect, suggesting that hypothermia and Mg²⁺ both regulate CBF by modulating Ca²⁺ influx into certain cells. CBF is mainly controlled by capillary diameter, and pericytes are the main regulators of capillary diameter [41]. TRPM8, a cold sensitive Ca²⁺ influx channel, has been detected in cerebral vessel and pericyte within tumors [42, 51]. The regulatory effects of hypothermia and Mg²⁺ on capillary diameter may be mediated by Ca²⁺ influx through TRPM8 on pericytes, which influences intracellular Ca²⁺ concentration and regulates their contraction state. The *in vitro* pericyte experiments in this study partially support this hypothesis, providing an explanation for the observed phenomenon *in vivo*. Future studies should aim to provide more direct *in vivo* evidence for this mechanism.

## The regulation effect of Mg²⁺ on Ca²⁺ homeostasis in different NVU cells

Mg²⁺ and Ca²⁺ are both divalent ions with similar chemical properties, suggesting that Mg²⁺ may compete with Ca²⁺ for the same non-selective cation channel on cerebral cells *in vivo*, generating antagonistic effects. Recent studies have provided some clues as to which channel Mg²⁺ act on in each NVU cell.

Several kinds of Ca²⁺ channels are expressed on the cell membranes of neurons. The Ca²⁺ overload caused by glutamate mediated N-methyl-D-aspartic acid (NMDA) receptor activation has been found to be the main mechanism contributing to neuronal I/R injury, and the blocking effect of Mg²⁺ on this channel was documented nearly 40 years ago [52, 53]. In recent years, with the discovery of the transient receptor potential (TRP) family channel proteins that regulate Ca²⁺ penetration, studies have found that the TRP melastatin 7 (TRPM7) may be activated *in vitro* by oxidative stress injury, which then induces neuronal death due to the occurrence of Ca²⁺ overload. In contrast, downregulation of TRPM7 in hippocampal neurons *in vivo* prevented I/R injury-induced neuronal death [54, 55]. It has also been reported that Mg²⁺ can block TRPM7 to reduce Ca²⁺ influx, thereby inhibiting the damage caused by oxidative stress [56]. Based on these findings, we speculated that the protective effect of Mg²⁺ may involve inhibition of the neuronal damage caused by TRPM7-triggered Ca²⁺ overload.

Currently, few studies have explored the regulation of Ca²⁺ overload in cerebral microvessel

ECs following AIS. In a recent study, it was found that TPPM2 influenced the occurrence of $Ca^{2+}$ overload in microvessel ECs after I/R injury, implying that BBB breakdown, neurological function deterioration, and inhibition of TRPM2 may rescue this adverse effect [57]. Moreover, another study showed that TRPM2 exhibited similar permeability for $Mg^{2+}$ and $Ca^{2+}$ [58]. Thus, the inhibitory effect of $Mg^{2+}$ on $Ca^{2+}$ overload in cerebral microvessel ECs identified in our study may be mediated by the blocking effect of $Mg^{2+}$ on TRPM2.

Voltage-gated $Ca^{2+}$ channels (VGCC) are the main channels for controlling the intracellular $Ca^{2+}$ concentration and contraction of microvessel diameter [59]. As the main regulator of cerebral microvascular diameter, the contraction of pericytes is also primarily regulated by VGCC. For example, a recent study showed that the L-type VGCC of cerebral pericytes was activated after I/R injury via the TMEM16A-mediated $Cl^-$ influx and the subsequent cell membrane depolarization, leading to pericyte contraction and cerebral "no-flow" phenomenon [60]. $Mg^{2+}$ can also inhibit VGCC [61], so we speculate that the inhibitory effect of $Mg^{2+}$ on pericyte contraction after I/R injury is mediated by VGCC on pericytes.

In summary, based on our results and previous research, we infer that $Mg^{2+}$, as a natural antagonist of $Ca^{2+}$, participates in $Ca^{2+}$ homeostasis in different NVU cells following I/R injury, however, considering that the main $Ca^{2+}$ regulatory pathways in each cell are different, the exact sites of action for $Mg^{2+}$ may also be inconsistent. In the future, well-designed experiments are advocated to investigate the regulation of $Ca^{2+}$ homeostasis in NVU cells in the context of I/R injury and explore the effects of $Mg^{2+}$ on its regulatory pathways.

### Perspectives

This study shows that $MgSO_4$ is a novel hypothermia infusion solution for promoting ischemic stroke recovery in rats. In the future, we hope to validate our findings in larger animals. Considering that hypothermia and $MgSO_4$ are common treatment methods, the combination therapy can be directly performed in clinical practice. Owing to the recent development of another new IA-SCI method using special instruments, IA-selective cooling autologous blood infusion (IA-SCAI) is expected to become a new approach for achieving targeted brain cooling [62, 63]. This technology can effectively address the challenge of long-term inability to maintain arterial cooling infusion due to capacity limitations. In the future, $Mg^{2+}$ could be added to the perfused cooling blood to potentially enhance its neuroprotective effects.

Mechanistically, diverse protective pathways are involved in the regulation of hypothermia and $Mg^{2+}$ effects. However, this study only explored selected superficial mechanisms, especially those associated with $Ca^{2+}$ in NVU cells. Further comprehensive and in-depth investigations are advocated.

## Conclusion

In summary, this study used $MgSO_4$ as a novel hypothermia infusion solution to assist in the synergistic inhibition of nerve and BBB damage, and reverse the early inhibitory effect of hypothermia on CBF, thereby synergistically protecting eventual CBF. Different $Ca^{2+}$ regulatory pathways were identified in various NVU cells, including neuron, mcirovessel ECs and pericytes, as possible mechanisms of the combination therapy.

## Abbreviations

AIS: acute ischemic stroke; BBB: blood-brain barrier; CBF: cerebral blood reflow; CCA: common carotid artery; CCK-8: cell counting kit-8; DMEM: Dulbecco's modified Eagle's medium; EB: Evans blue; ECA: external carotid artery; ECs: endothelial cells; FBS: fetal bovine serum; IA-SCAI: intra-arterial selective cooling autologous blood infusion; IA-SCMI: intra-arterial selective cooling infusion solution; IA-SCSI: intra-arterial selective cooling saline infusion; IA-SI: intra-arterial selective infusion; ICA: internal carotid artery; I/R: ischemia/reperfusion; LDH: lactic dehydrogenase; MABP: mean arterial blood pressure; MCAO: middle cerebral artery occlusion; $MgCl_2$: magnesium chloride; $MgSO_4$: magnesium sulfate; mNSS: modified neuropathy symptom score; NMDA: N-methyl-D-aspartic acid; NVUs: neurovascular units; OGD/R: oxygen-glucose deprivation/reoxygenation; PBS: phosphate-buffered saline; $pCO_2$: arterial carbon dioxide partial pressure; PI: propyl iodide; $pO_2$: arterial oxygen partial pressure; RT: room temperature; SD: Sprague-Dawley; TRP: transient receptor potential; TRPM7: transient receptor potential melastatin 7; TTC: triphenyltetrazolium chloride; VGCC: Voltage-gated $Ca^{2+}$ channels.

## Supplementary Material

Supplementary figures and table.
https://www.thno.org/v15p1896s1.pdf

## Acknowledgements

## Ethics committee approval

All experimental procedures were approved by Institutional Animal Investigation Committee of Capital Medical University, which made sure that all animal treatments properly followed the National Institutes of Health's guidelines for the Care and Use of Laboratory Animals.

## Data availability

Data available on request from the authors.

## Author contributions

**Yang Zhang:** Conceptualization; formal analysis; investigation; methodology; software; writing – original draft; **Miaowen Jiang:** methodology; **Ming Wei:** Formal analysis; **Chuanjie Wu:** Investigation; **Yiming Huang:** Investigation; **Baoying Song:** Methodology; **Yi Xu:** Software; **Hongkang Zhang:** Methodology; **Yunong Shen:** Investigation; **Di Wu:** Writing – review and editing; **Yufeng Zheng:** Methodology; writing – review and editing; **Ming Li:** Methodology; writing – review and editing; **Xunming Ji:** Conceptualization; project administration; writing – review and editing.

## Competing Interests

The authors have declared that no competing interest exists.

## References

1. Powers WJ. Acute Ischemic Stroke. N Engl J Med. 2020; 383: 252-60.
2. Eren F, Yilmaz SE. Neuroprotective approach in acute ischemic stroke: A systematic review of clinical and experimental studies. Brain Circ. 2022; 8: 172-9.
3. Lauzier DC, Kansagra AP. Thrombectomy in Acute Ischemic Stroke. N Engl J Med. 2022; 386: 1351.
4. Jiang X, Hu Y, Wang J, Ma M, Bao J, Fang J, et al. Outcomes and risk factors for infection after endovascular treatment in patients with acute ischemic stroke. CNS Neurosci Ther. 2024; 30: e14753.
5. Yenari MA, Han HS. Neuroprotective mechanisms of hypothermia in brain ischaemia. Nature Reviews Neuroscience. 2012; 13: 267-78.
6. Lyden PD, Lamb J, Kothari S, Toossi S, Boitano P, Rajput PS. Differential effects of hypothermia on neurovascular unit determine protective or toxic results: Toward optimized therapeutic hypothermia. J Cereb Blood Flow Metab. 2019; 39: 1693-709.
7. Wu L, Wu D, Yang T, Xu J, Chen J, Wang L, et al. Hypothermic neuroprotection against acute ischemic stroke: The 2019 update. Journal of Cerebral Blood Flow and Metabolism : Official Journal of the International Society of Cerebral Blood Flow and Metabolism. 2020; 40: 461-81.
8. Diprose WK, Morgan CA, Wang MT, Diprose JP, Lin JC, Sheriff S, et al. Active conductive head cooling of normal and infarcted brain: A magnetic resonance spectroscopy imaging study. J Cereb Blood Flow Metab. 2022; 42: 2058-65.
9. Chen X, Xu S, Li M, Wu D, Ji X. Transnasal cooling: New prospect of selective hypothermia in acute ischemic stroke. J Cereb Blood Flow Metab. 2024; 44: 310-312.
10. Li M, Gao Y, Jiang M, Zhang H, Zhang Y, Wu Y, et al. Dual-sized hollow particle incorporated fibroin thermal insulating coatings on catheter for cerebral therapeutic hypothermia. Bioact Mater. 2023; 26: 116-27.
11. Gao Y, Li M, Jiang M, Zhang Y, Ji X. A narrative review of intravascular catheters in therapeutic hypothermia. Brain Circ. 2024; 10: 11-20.
12. Luan X, Li J, McAllister JP, Diaz FG, Clark JC, Fessler RD, et al. Regional brain cooling induced by vascular saline infusion into ischemic territory reduces brain inflammation in stroke. Acta Neuropathol. 2004; 107: 227-34.
13. Wu D, Fu Y, Wu L, Huber M, Chen J, Yao T, et al. Reperfusion plus Selective Intra-arterial Cooling (SI-AC) Improve Recovery in a Nonhuman Primate Model of Stroke. Neurotherapeutics. 2020; 17: 1931-9.
14. Wu C, Zhao W, An H, Wu L, Chen J, Hussain M, et al. Safety, feasibility, and potential efficacy of intraarterial selective cooling infusion for stroke patients treated with mechanical thrombectomy. J Cereb Blood Flow Metab. 2018; 38: 2251-60.
15. Roche M, Chaigneau E, Rungta RL, Boido D, Weber B, Charpak S. In vivo imaging with a water immersion objective affects brain temperature, blood flow and oxygenation. Elife. 2019; 8: e47324.
16. Zausinger S, Schöller K, Plesnila N, Schmid-Elsaesser R. Combination drug therapy and mild hypothermia after transient focal cerebral ischemia in rats. Stroke. 2003; 34: 2246-51.
17. Campbell K, Knuckey NW, Brookes LM, Meloni BP. Efficacy of mild hypothermia (35° C) and moderate hypothermia (33° C) with and without magnesium when administered 30min post-reperfusion after 90min of middle cerebral artery occlusion in Spontaneously Hypertensive rats. Brain Res. 2013; 1502: 47-54.
18. Song B, Jiang M, Zhang Y, Xu Y, Wu C, Wu D, et al. Research hotpots and frontier trends of neuroprotective effects of magnesium from 1999 to 2023: A bibliometric analysis. CNS Neurosci Ther. 2024; 30: e14597.
19. Lin J-Y, Chung S-Y, Lin M-C, Cheng F-C. Effects of magnesium sulfate on energy metabolites and glutamate in the cortex during focal cerebral ischemia and reperfusion in the gerbil monitored by a dual-probe microdialysis technique. Life Sci. 2002; 71: 803-11.
20. Shogi T, Oono H, Nakagawa M, Miyamoto A, Ishiguro S, Nishio A. Effects of a low extracellular magnesium concentration and endotoxin on IL-1beta and TNF-alpha release from, and mRNA levels in, isolated rat alveolar macrophages. Magnesium Res. 2002; 15: 147-52.
21. Kaya M, Küçük M, Kalayci RB, Cimen V, Gürses C, Elmas I, et al. Magnesium sulfate attenuates increased blood-brain barrier permeability during insulin-induced hypoglycemia in rats. Can J Physiol Pharmacol. 2001; 79: 793-8.
22. Berthon N, Laurant P, Fellmann D, Berthelot A. Effect of magnesium on mRNA expression and production of endothelin-1 in DOCA-salt hypertensive rats. J Cardiovasc Pharmacol. 2003; 42: 24-31.
23. Phillips KF, Deshpande LS, DeLorenzo RJ. Hypothermia reduces calcium entry via the N-methyl-D-aspartate and ryanodine receptors in cultured hippocampal neurons. Eur J Pharmacol. 2013; 698: 186-92.
24. Phillips KF, Deshpande LS, DeLorenzo RJ. Hypothermia Reduces Mortality, Prevents the Calcium Plateau, and Is Neuroprotective Following Status Epilepticus in Rats. Front Neurol. 2018; 9: 438.
25. Longa EZ, Weinstein PR, Carlson S, Cummins R. Reversible middle cerebral artery occlusion without craniectomy in rats. Stroke. 1989; 20: 84-91.
26. Chen J, Fredrickson V, Ding Y, Jiang L, Luo Y, Ji X. The effect of a microcatheter-based selective intra-arterial hypothermia on hemodynamic changes following transient cerebral ischemia. Neurol Res. 2015; 37: 263-8.
27. Song W, Wu Y-M, Ji Z, Ji Y-B, Wang S-N, Pan S-Y. Intra-carotid cold magnesium sulfate infusion induces selective cerebral hypothermia and neuroprotection in rats with transient middle cerebral artery occlusion. Neurol Sci. 2013; 34: 479-86.
28. Duan J, Wu D, Huber M, Shi J, An H, Wei W, et al. New Endovascular Approach for Hypothermia With Intrajugular Cooling and Neuroprotective Effect in Ischemic Stroke. Stroke. 2020; 51: 628-36.
29. Ding Y, Yao B, Zhou Y, Park H, McAllister JP, Diaz FG. Prereperfusion flushing of ischemic territory: a therapeutic study in which histological and behavioral assessments were used to measure ischemia-reperfusion injury in rats with stroke. J Neurosurg. 2002; 96: 310-9.
30. Chen J, Sanberg PR, Li Y, Wang L, Lu M, Willing AE, et al. Intravenous administration of human umbilical cord blood reduces behavioral deficits after stroke in rats. Stroke. 2001; 32: 2682-8.
31. Hamm RJ, Pike BR, O'Dell DM, Lyeth BG, Jenkins LW. The rotarod test: an evaluation of its effectiveness in assessing motor deficits following traumatic brain injury. J Neurotrauma. 1994; 11: 187-96.
32. Chen J, Li Y, Wang L, Zhang Z, Lu D, Lu M, et al. Therapeutic benefit of intravenous administration of bone marrow stromal cells after cerebral ischemia in rats. Stroke. 2001; 32: 1005-11.

33. Esposito E, Ahn BJ, Shi J, Nakamura Y, Park JH, Mandeville ET, et al. Brain-to-cervical lymph node signaling after stroke. Nat Commun. 2019; 10: 5306.
34. Yue Y, Chen P, Ren C. Piezo1 Modulates Neuronal Autophagy and Apoptosis in Cerebral Ischemia-Reperfusion Injury Through the AMPK-mTOR Signaling Pathway. Neurochem Res. 2024; 50: 32.
35. Su EJ, Fredriksson L, Geyer M, Folestad E, Cale J, Andrae J, et al. Activation of PDGF-CC by tissue plasminogen activator impairs blood-brain barrier integrity during ischemic stroke. Nat Med. 2008; 14: 731-7.
36. Shi Y, Zhang L, Pu H, Mao L, Hu X, Jiang X, et al. Rapid endothelial cytoskeletal reorganization enables early blood-brain barrier disruption and long-term ischaemic reperfusion brain injury. Nat Commun. 2016; 7: 10523.
37. Allen LA, Terashvili M, Gifford A, Lombard JH. Evaluation of Cerebral Blood Flow Autoregulation in the Rat Using Laser Doppler Flowmetry. J Visualized Exp. 2020; (155).
38. Gullotta GS, De Feo D, Friebel E, Semerano A, Scotti GM, Bergamaschi A, et al. Age-induced alterations of granulopoiesis generate atypical neutrophils that aggravate stroke pathology. Nat Immunol. 2023; 24: 925-40.
39. Bonache MÁ, Llabrés PJ, Martín-Escura C, De la Torre-Martínez R, Medina-Peris A, Butrón L, et al. Phenylalanine-Derived $\beta$-Lactam TRPM8 Modulators. Configuration Effect on the Antagonist Activity. Int J Mol Sci. 2021; 22: 2370.
40. Nazıroğlu M, Ozgül C. Effects of antagonists and heat on TRPM8 channel currents in dorsal root ganglion neuron activated by nociceptive cold stress and menthol. Neurochem Res. 2012; 37: 314-20.
41. Hall CN, Reynell C, Gesslein B, Hamilton NB, Mishra A, Sutherland BA, et al. Capillary pericytes regulate cerebral blood flow in health and disease. Nature. 2014; 508: 55-60.
42. Fedinec AL, Liu J, Zhang R, Harsono M, Pourcyrous M, Parfenova H. The cold receptor TRPM8 activation leads to attenuation of endothelium-dependent cerebral vascular functions during head cooling. J Cereb Blood Flow Metab. 2021; 41: 2897-906.
43. Marinov MB, Harbaugh KS, Hoopes PJ, Pikus HJ, Harbaugh RE. Neuroprotective effects of preischemia intraarterial magnesium sulfate in reversible focal cerebral ischemia. J Neurosurg. 1996; 85: 117-24.
44. Zhu H, Meloni BP, Bojarski C, Knuckey MW, Knuckey NW. Post-ischemic modest hypothermia (35 degrees C) combined with intravenous magnesium is more effective at reducing CA1 neuronal death than either treatment used alone following global cerebral ischemia in rats. Exp Neurol. 2005; 193: 361-8.
45. Rahman SU, Canpolat FE, Oncel MY, Evli A, Dilmen U, Parappil H, et al. Multicenter Randomized Controlled Trial of Therapeutic Hypothermia Plus Magnesium Sulfate Versus Therapeutic Hypothermia Plus Placebo in the Management of Term and Near-Term Infants with Hypoxic Ischemic Encephalopathy (The Mag Cool Study): A Pilot Study. J Clin Neonatol. 2015; 4: 158-63.
46. Han Y, Han Z, Huang X, Li S, Jin G, Feng J, et al. An injectable refrigerated hydrogel for inducing local hypothermia and neuroprotection against traumatic brain injury in mice. J Nanobiotechnol. 2024; 22: 251.
47. Kurisu K, Abumiya T, Nakamura H, Shimbo D, Shichinohe H, Nakayama N, et al. Transarterial Regional Brain Hypothermia Inhibits Acute Aquaporin-4 Surge and Sequential Microvascular Events in Ischemia/Reperfusion Injury. Neurosurgery. 2016; 79: 125-34.
48. Zhang Q, Song Q, Yu R, Wang A, Jiang G, Huang Y, et al. Nano-Brake Halts Mitochondrial Dysfunction Cascade to Alleviate Neuropathology and Rescue Alzheimer's Cognitive Deficits. Adv Sci. 2023; 10: e2204596.
49. León J, Acurio J, Bergman L, López J, Karin Wikström A, Torres-Vergara P, et al. Disruption of the Blood-Brain Barrier by Extracellular Vesicles From Preeclampsia Plasma and Hypoxic Placentae: Attenuation by Magnesium Sulfate. Hypertension. 2021; 78: 1423-33.
50. Xu S-Y, Hu F-Y, Ren L-J, Chen L, Zhou Z-Q, Zhang X-J, et al. Dantrolene enhances the protective effect of hypothermia on cerebral cortex neurons. Neural Regener Res. 2015; 10: 1279-85.
51. Li X, Qi Q, Li Y, Miao Q, Yin W, Pan J, et al. TCAF2 in Pericytes Promotes Colorectal Cancer Liver Metastasis via Inhibiting Cold-Sensing TRPM8 Channel. Adv Sci. 2023; 10: e2302717.
52. Nowak L, Bregestovski P, Ascher P, Herbet A, Prochiantz A. Magnesium gates glutamate-activated channels in mouse central neurones. Nature. 1984; 307: 462-5.
53. Shindo Y, Fujimoto A, Hotta K, Suzuki K, Oka K. Glutamate-induced calcium increase mediates magnesium release from mitochondria in rat hippocampal neurons. J Neurosci Res. 2010; 88: 3125-32.
54. Aarts M, Iihara K, Wei W-L, Xiong Z-G, Arundine M, Cerwinski W, et al. A key role for TRPM7 channels in anoxic neuronal death. Cell. 2003; 115: 863-77.
55. Sun H-S, Jackson MF, Martin LJ, Jansen K, Teves L, Cui H, et al. Suppression of hippocampal TRPM7 protein prevents delayed neuronal death in brain ischemia. Nat Neurosci. 2009; 12: 1300-7.
56. Inoue H, Murayama T, Tashiro M, Sakurai T, Konishi M. Mg(2+)- and ATP-dependent inhibition of transient receptor potential melastatin 7 by oxidative stress. Free Radic Biol Med. 2014; 72: 257-66.
57. Zong P, Feng J, Li CX, Jellison ER, Yue Z, Miller B, et al. Activation of endothelial TRPM2 exacerbates blood-brain barrier degradation in ischemic stroke. Cardiovasc Res. 2024; 120: 188-202.
58. Xia R, Mei Z-Z, Mao H-J, Yang W, Dong L, Bradley H, et al. Identification of pore residues engaged in determining divalent cationic permeation in transient receptor potential melastin subtype channel 2. J Biol Chem. 2008; 283: 27426-32.
59. Hashitani H, Lang RJ. Spontaneous activity in the microvasculature of visceral organs: role of pericytes and voltage-dependent Ca(2+) channels. J Physiol. 2016; 594: 555-65.
60. Korte N, Ilkan Z, Pearson CL, Pfeiffer T, Singhal P, Rock JR, et al. The Ca2+-gated channel TMEM16A amplifies capillary pericyte contraction and reduces cerebral blood flow after ischemia. J Clin Invest. 2022; 132: e154118.
61. AlShanableh Z, Ray EC. Magnesium in hypertension: mechanisms and clinical implications. Front Physiol. 2024; 15: 1363975.
62. Jiang M, Zhang Y, Gao Y, Xu S, Qi Z, Wu C, et al. A computationally guided study of a blood heat exchanger and the construction of an extracorporeal circulation system for selective brain cooling. Cell Rep Phys Sci. 2024; 5: 102029.
63. Chen J, Xu S, Lee H, Wu L, He X, Zhao W, et al. Hypothermic neuroprotection by targeted cold autologous blood transfusion in a non-human primate stroke model. Sci Bull (Beijing). 2023; 68: 1556-66.